



Investigation in Hydroxyapatite After Cationic Substitution with Neodymium and Magnesium

Suha Q. AL-Shahrabalee^{1*}, Hussein Alaa Jaber²

^{1,2}Department of Materials Engineering, University of Technology-Iraq, Baghdad, 10001, Iraq

*Corresponding author: Suha Q. AL-Shahrabalee, Department of Materials Engineering, University of Technology-Iraq, Baghdad, 10001, Iraq, Email: mae.19.09@grad.uotechnology.edu.iq

Submitted: 10 January 2023; Accepted: 23 February 2023; Published: 22 March 2023

ABSTRACT

The development of biomimetic nanomaterials is paying increasing attention to compositional modeling. Hydroxyapatite is among the essential biomaterials for orthopedic and dental applications because the mineral component of bone is chemically similar to hydroxyapatite-based biomaterials. In this study, hydroxyapatite was cationically substituted with neodymium and magnesium via adopting a wet chemical precipitation technique to produce the analogous inorganic phase of bone and make their structure therapeutically fight pathogens. The morphological and compositional characteristics were tested by utilizing FTIR, XRD, and FESEM which revealed the presence of the HA phase with great compositional purity of the produced nanomaterial and obvious change in crystallinity, lattice properties, morphology, and particle shape. Along with that, the biological tests exhibited improvement in antitumor activity and biocompatibility which were examined with depend on MG63 and WRL68 cell lines, respectively. The presence of neodymium with magnesium in the HA structure makes it has antibacterial and fungicide activity.

Keywords: *Substitution; hydroxyapatite; orthopedic; antitumor*

1. INTRODUCTION

The clinical outcomes demonstrate the need for improved and innovative biomaterials which is in direct contact with bodily fluids and human tissues to satisfy the basic requirements of orthopedic devices and correctly work over the long term [1][2][3]. One of the most vital and exciting areas of research in the field of materials science for scientific advancement in the twenty-first century is the development of innovative bioactive materials with versatility for orthopedic applications. Artificial orthopedic alternatives become more significant during the past few decades as a result of the rise in bone abnormalities and joint degeneration brought on

by an aging global population [4].

Calcium phosphate compounds, such as hydroxyapatite (HA), are frequently used as implants and coating for orthopedic purposes because of their outstanding biocompatibility, osteoconductive behavior, and chemical stability in the living system [5]. It is regarded as a bioactive material having the formula $\text{Ca}_{10}(\text{PO}_4)_6(\text{OH})_2$ and contains Ca/P components, improves the bone/implant bonding capabilities due to the compositional resemblance to that of the bones, which make up the majority of the bone's inorganic component, HA coatings promote the bone ingrowth as well as improved osseointegration [6].

Though, Synthetic HA cannot be used to create load-bearing bulk implants or prostheses that are mechanically secure due to its weak mechanical qualities (low fracture toughness, poor tensile strength). Therefore, the use of HA has been restricted to fillers and coatings of metallic biomaterials for the bio-functionalization or porous scaffolds as bone grafts [7]. HA can be directly employed in bone tissue [8] or its characteristics can be modified for later usage by adding other metallic or nonmetallic dopants [9]. Depending on the dopant's characteristics, the substitution improves the modified HA's qualities. Magnesium, silver, cobalt, lithium, zinc, strontium, cerium, hafnium, and neodymium are a few examples of these dopants which can improve the quality and application range of HA by having distinct beneficial effects on it [10]. The hexagonal unit cell of hydroxyapatite contains ten Ca²⁺ ions, six (PO₄³⁻) ions, and two (OH⁻) ions. Ca(I) and Ca(II) are two distinct cation sites, where the big cations can be hosted at the Ca(II) site, while small cations and limited amounts of bigger cations can be hosted at the Ca(I) site [11]. The solubility of substituted HA is typically enhanced by replacing certain Ca²⁺ ions with other cations. This characteristic could be explained by the altered crystallinity and crystallite size, as well as the disruption of the HA lattice caused by lattice strain brought on by the inclusion of foreign ions of various sizes, which affects their stability. Moreover, some of these ions may simply be adsorbed, at least in part, on the surface of HA NPs, making them easier to remove from a liquid immersion [5].

In biomedical applications, rare earth elements are interesting prospects for biodegradable devices. The biocompatibility test of calcium phosphate compounds containing Nd on the L929 fibroblast cell line showed that cell viability was higher than 90% with no impact on cell growth. Presence of Nd in calcium phosphate compounds can deliver anticancer drugs with excellent selectivity and enable fluorescence imaging, which would be a huge development in cancer therapy [12]. Magnesium is a crucial element that the human body needs. It is also one of the elements that can be used as a cationic replacement for calcium in the HA lattice and are

a substantial trace element in human bones. Above all else, maintaining the proper Mg to Ca ratio is crucial for both treating and preventing osteoporosis. Mg is known to increase cellular adhesion to the substrate as well as osteoblast-like cell proliferation, calcification, and angiogenic activity. Thus, it is essential to add Mg to synthetic HA for a number of reasons, including improved bioactivity.

This study aimed to prepare hydroxyapatite substituted with neodymium and magnesium through the wet chemical precipitation method and utilize the new structure to improve the biological properties such as the antibacterial and fungicide activity in addition to increasing the biocompatibility and antitumor activity due to the presence of substituted elements.

2. MATERIALS AND METHOD

2.1. Sample preparation

Wet chemical precipitation is regarded as a method of hydroxyapatite production that requires aqueous solutions to be used wherein Ca and P ions' chemical interactions take place at a regulated pH and temperature. The synthesis is accomplished by substituting 5% from Ca ions with neodymium and magnesium. The exact preparation highly depends on theoretical calculations to adjust the molar ratio for substituted HA (Nd-Mg/HA) and make it equal to the molar ratio of bone (1.67) according to the following equation:

$$\frac{\text{Ca} + \text{Nd} + \text{Mg}}{\text{P}} = \frac{0.06346 + 0.00167 + 0.00167}{0.03999} = 1.67$$

The source of nitrate ions contains (0.167M) from hydrated nitrate salts which included, calcium nitrate (CaH₈N₂O₁₀), neodymium nitrate (H₁₂N₃NdO₁₅), and magnesium nitrate (H₁₂MgN₂O₁₂) which is then mixed (by dropping) with (0.1M) of a solution containing phosphorous ions prepared from (NH₃)₂HPO₄ salts and its pH was adjusted to above 10 by using ammonia.

The chemical reactions take place at controlled pH and temperature (70°C). After a few hours, the pH was raised to about 11 gradually and The

heating was turned off to give the solution adequate time (one day) to age at room temperature.

The most frequent reaction is the neutralization reaction that results in the production of water as a byproduct which was removed via filtering and the remaining powder splashed repeatedly through deionized H₂O, dried at 100°C for about 8 hours to obtain bioceramic peels as indicated in Fig. (1). Finally, this peels where sintered at 800°C and it was ground by a hand mortar.



FIG. 1: Peels of neodymium and magnesium substituted hydroxyapatite.

2.2. Specimens characterization tests

2.2.1. Fourier Transform-Infrared Spectroscopy (FTIR)

With the use of potassium bromide pellets, FTIR spectroscopy was performed at a spectral range from 599.8 cm⁻¹ to 3996.3 cm⁻¹ to identify the functional groups of Nd-Mg/HA using a (Bruker Tensor 27 IR, Germany) instrument. The test sample's whole functional groups are represented by the FTIR spectra that are acquired using the transmittance mode.

2.2.2. X-Ray Diffraction (XRD)

Using the Philips X'Pert X-ray PRO (Holland) with the radiation of CuK α ($\lambda=1.5405$), XRD technique was used to confirm the evolution of substituted HA powder and its component. In order to identify the HA phase and substituted elements, the experimental XRD patterns were compared to those of the X'Pert HighScore Plus and drawn at 2θ from 10° to 80° with a step of 0.05° point/second.

2.2.3. Field Emission-Scanning Electron Microscope (FE-SEM) and Energy Dispersive Spectroscopy (EDS)

In addition to EDS with mapping, which was utilized to identify the composition of the produced powder and determine the elemental distribution, FE-SEM was employed to study the microstructure of Nd-Mg/HA. Both techniques were carried out using a Zeiss Sigma 300-HV (Germany).

2.2.4. Antibacterial activity

The prepared powder was tested using an agar well diffusion assay for its antibacterial properties against *E. coli*, *S. mutans*, *S. aureus*, *S. epidermidis*, in addition to examining its behavior against fungi (*Candida albicans*) [13][14]. 20mL from Muller-Hinton (MH) agar added aseptically in sterilized Petri dishes. By a sterilized wire loop, the microorganism from their stock cultures were extracted [15]. Cultured plates containing the test organisms and the samples stayed in an incubation period overnight at a temperature of 37°C, then measured the average diameter of the inhibitory zones [16].

2.2.5. Biocompatibility and antitumor activity

A key characteristic of biocompatible materials is that they do not have an adverse toxic or immunological reaction when they are exposed to the body or bodily fluids, which is regarded as a crucial property for biomaterial. On the other side, the biomaterial should be resistant to a pathogen such as cancer diseases. Both these properties were investigated by adopting the normal cell line (WRL68) and cancer cell line (MG63). These cell lines were cultured in the laboratory according to the standard conditions and the results were analyzed statistically by Graph Pad Prism.

3. RESULTS AND DISCUSSIONS

3.1. Fourier Transform Infrared Spectroscopy test (FTIR)

Table (1) and Fig. (2) illustrate the FTIR spectra of the prepared powder, which show the primary functional groups of HA in addition to other minor functional groups. The two essential

functional groups of HA were observed where the vibrational mode of the hydroxyl (OH)- and (PO₄)₃⁻ groups can be recognized at different bands. The 5% of Ca ions that substituted with neodymium and magnesium doesn't affect the transmittance of (O-P-O) stretching mode and the band of (PO₄)₃⁻ group. On the other hand, the presence of the (HPO₄)₂⁻ group in the substituted HA sample indicates calcium deficiency, which

is the feature of substituted HA [17]. Some carbonate ion vibrations have large and frail shoulders, indicating the carbonate ions (CO₃)₂⁻ presence but only traces inside the substituted HA structure. However, They may actually increase the bioactivity of HA since the bone mineral phase is carbonated, thus not being a reason for concern [18].

TABLE 1: Chemical groups of the Nd-Mg/HA.

Chemical groups	Wavenumber (cm-1)	General information	Ref.
OH-	630	Prove the formation of HA as one of the essential functional groups in hydroxyapatite	[17]
	3571		[19] [20]
PO ₄ ³⁻	963	* Prove formation of HA	[21][17]
	1023	* Vibrational mode	[18][22]
	1090	v1 → 963cm-1 v3 → 1023cm-1	[23][24] [25]
HPO ₄ ²⁻	873	* This group results from some of the PO ₄ groups that were close to the OH ions * Distinguishing HA when calcium deficiency	[26] [27]
CO ₃ ²⁻	1416	* Arise from the adsorption of atmospheric carbon dioxide	[28][25]
	1456	* The low intensity of CO ₃ ²⁻ indicates a greater assay degree	[23][29] [30]

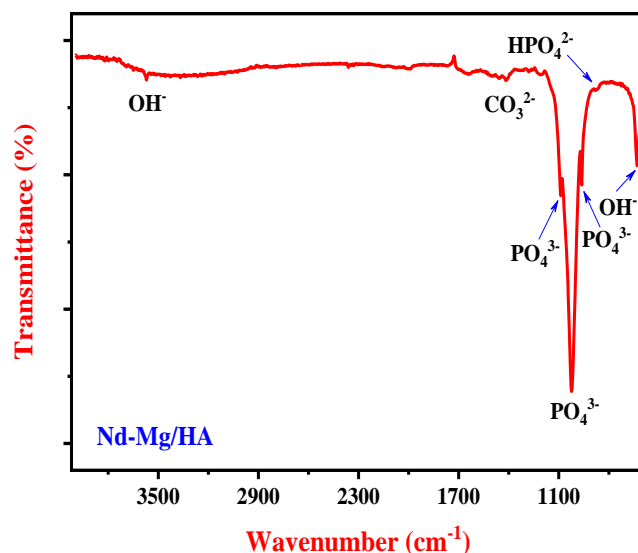


FIG 2: FTIR spectra of neodymium and magnesium substituted hydroxyapatite.

3.2. XRD

The XRD pattern of Nd-Mg/HA in Table (2) and Fig. (3) illustrates the peaks of HA at 26.115°, 28.328°, 32.032°, 34.346°, 40.053°, 42.319°, 44.064°, 46.966°, 49.771°, 53.401°, 64.254°, 71.928°, and 77.256° according to reference code (00-001-1008). Substituted metals were noticed in the XRD pattern in addition to hydroxyapatite, where the peaks 28.328°, 29.154°, 32.032°, 34.346°, 35.710°, 42.319°, 44.064°, 48.297°, 49.771°, 60.463°, 64.254°, 71.928°, and 77.256° matches the Nd reference code (00-039-0914),

(01-089-2922), (01-089-5328), and (01-089-5330), whereas the peaks 32.032°, 34.346°, 48.297°, and 77.256° were found that belongs to Mg according to reference code (00-004-0770). When contrasting these outcomes with hydroxyapatite without substitution, it was found that there is a little shaft in HA peaks where the peaks of non-substituted HA appear at 2θ values 26.098°, 31.978°, 34.284°, 42.276°, 43.996°, 46.934°, 49.643°, 53.322°, 64.234°, and 72.117° [9].

TABLE 2: X- ray diffraction results of Nd-Mg/HA.

Peak position 2θ (°)	Interplaner spacing d (Å)	FWHM (°)	Miller indices (hkl)
26.1152	3.41228	0.2952	002
28.3284	3.15052	0.2952	012
32.032	2.7942	0.3936	112
34.3461	2.61106	0.246	022
40.0534	2.25119	0.3936	221
42.3194	2.13574	0.3936	032
44.0636	2.05517	0.3936	040
46.9657	1.93472	0.1968	222
49.7714	1.83204	0.3444	123
53.4009	1.71576	0.2952	004
64.2535	1.44969	0.3936	233
71.9279	1.31273	0.984	044
77.2563	1.23393	0.72	153

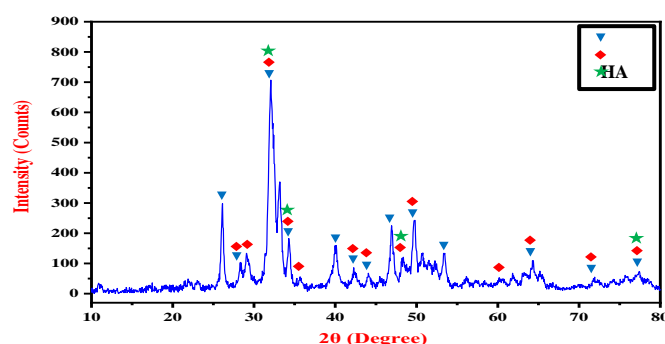


FIG 3: Essential peaks for the Nd-Mg/HA.

If compared the lattice parameter of Nd-Mg/HA (a , b = 9.492Å and c = 6.825Å) to those found in original hydroxyapatite (a , b = 9.445Å and c = 6.829Å), it was found that all the cations which replaced calcium ions in the HA lattice may cause very little changes in lattice parameters due

to the difference between the ionic radius of neodymium, magnesium, and calcium [9].

The crystallinity of substituted hydroxyapatite reduced after substitution if compared with HA because the metal substitution in the HA lattice is

responsible for the peaks broadening brought on by a decrease in size of the crystal and a rise in lattice disorder as it is clear for the value of lattice strain. Additionally, it is possible to classify the

hydroxyapatite samples as nano-HA based on the crystallite sizes determined employing the Scherrer equation [31].

TABLE 3: Lattice parameter of Hydroxyapatite [9] and Nd-Mg/HA.

Prepared material	Lattice parameter			Crystallite size (nm)	Lattice strain
	a (Å)	b (Å)	c (Å)		
HA	9.445	9.445	6.829	43.88	0.003
Nd-Mg/HA	9.492	9.492	6.825	21.84	0.006

The structure of HA and substituted HA was drawn based on the findings of an XRD test, using diamond software in order to investigate the change in structure. It is evident that substituted elements take some Ca positions after substitution as indicated in Fig. 4 (a) and (b).

There are two Ca sites accessible for cationic substitution, Ca(1) and Ca(2), with some metals favoring one over the other. It is reasonable to anticipate that the physical, biological, and chemical characteristics of HA will be affected by the ion exchange of Ca²⁺ by either trivalent bivalent ions. For instance, magnesium may easily replace calcium in biological

hydroxyapatite, and magnesium increases the bioactivity of HA by stimulating the activity of osteoblasts.

Lanthanides are known to have a strong affinity for HA. The donor atoms and ionic radii of lanthanide ions are comparable to those of Ca²⁺ ions. Where the ionic radius of Nd is 98.3pm which is regarded as very comparable to Ca (100pm).

Although it is generally known that ions of lanthanide can replace Ca ions in the bone mineral HA, its strength and the mechanisms affecting binding are not well understood [32].

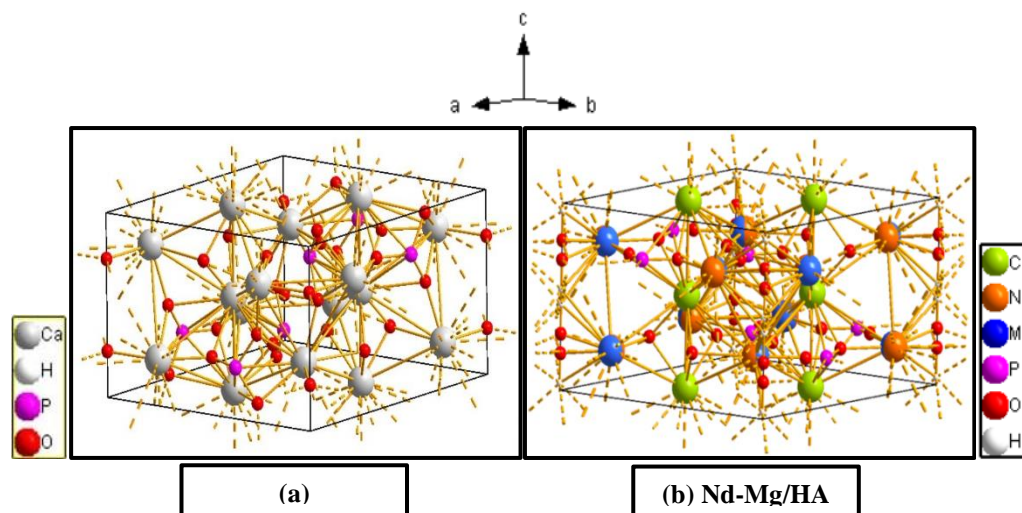


FIG 4: Structure of (a) HA and (b) Nd-Mg/HA.

3.3. Microstructure and elemental composition analysis by FE-SEM and EDS with mapping

Substitution of hydroxyapatite with multiple elements (Nd and Mg) associated with alteration in the morphology of nano-hydroxyapatite. Nd's

presence causes the generation of rod-like particles [33] interlaced with the elongated particles of hydroxyapatite which was induced by the substitution of Ca ion with Mg [34]. This change was obvious in Fig. (5) with 100nm

resolution and 100.00KX magnification which also indicate the particle size which ranged between 46.73nm and 83.66nm. In addition, the main factor that gives hydroxyapatite its

morphology is all the factors related to the preparation of hydroxyapatite, including temperature, pH, and the elements involved in the preparation of hydroxyapatite [35].

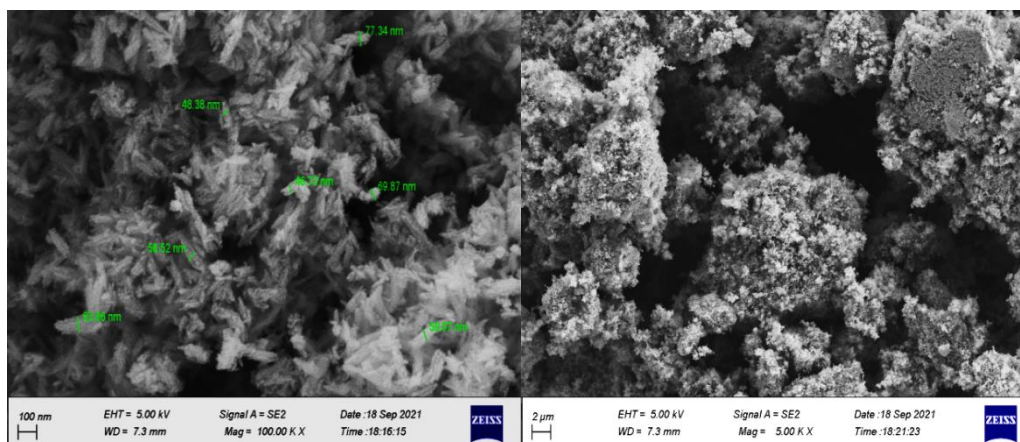


FIG 5: FE-SEM images of Nd-Mg/HA.

The bioactive layer of any biomaterial must have an elemental composition that is compatible with the content of the bone. The features of calcium phosphate compounds that can be used in surgical applications are determined by the Ca/P ratio, which is a crucial component [36]. The chemical composition of substituted HA was explained in Fig. (6) where the EDS test shows the presence of essential elements of hydroxyapatite with Nd and Mg. From the attached tables in fig. (6), it is obvious that the ratio of Ca/P was changed after substitution to

Ca+M/P and it was 1.64 which regarded very close to that of natural bone. The two key factors that affect the molar ratio (Ca/P) were the pH value and sintering temperature [37] where substituted HA was prepared at a pH of 11 and sintered at 800°C. Thus, the theoretical calculations of the Ca/P molar ratio will be very close to the practical results if the basic factors of the reaction are controlled correctly. The distribution of all elements was explained in Fig. (7).

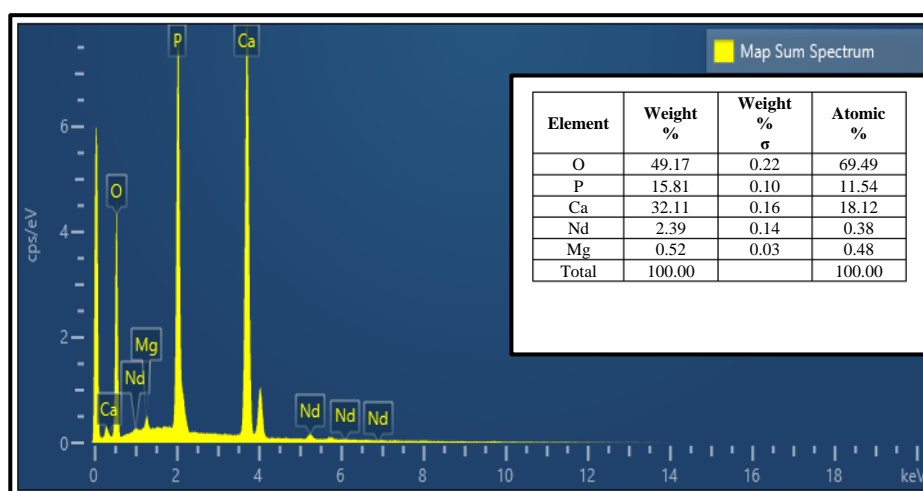


FIG 6: EDS analysis to explain the composition of Nd-Mg/HA.

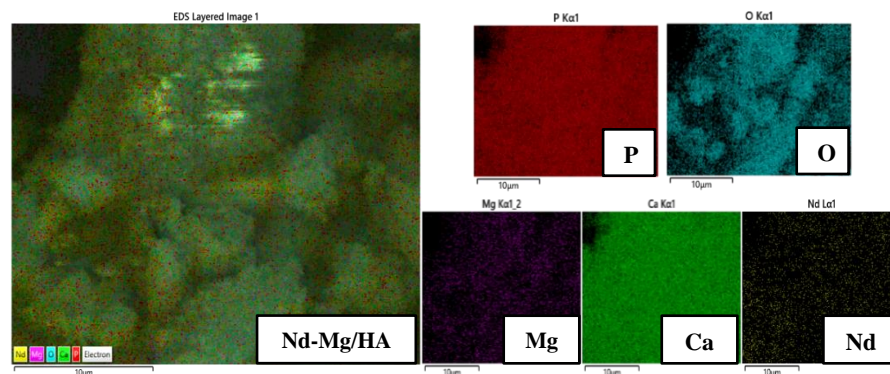


FIG 7: Elemental distribution of Nd-Mg/HA.

3.4. Antibacterial activity

It is obvious from Fig. (8) that substituted HA were resistant to gram-positive bacteria, gram-negative bacteria, and fungi with maximum inhibitory influence against *S. aureus* and *S. mutans*. Commercial hydroxyapatite doesn't exhibit antimicrobial activity but the state of hydroxyapatite preparation, purity, and substituted elements plays a significant influence in determining its efficacy against microorganisms.

Nano size of substituted HA has better engagement with the microbial target because of the nanoparticles' wide surface area of contact with microbial cells. Also, the suppression of bacterial growth via different shapes of nanoparticles demonstrated that the antibacterial effectiveness of the nanoparticles depending on the nanoparticles' shape [38].

Elements of rare earth including Nd are regarded as toxic to bacteria and fungi. In the existence of rare earth elements, many filamentous fungi hyphae have abnormal morphological features. Multiple terminal branching, swelling, lateral branching, and the breaking of hyphal strands by a mechanism analogous to plasmolysis are

among these changes. Asexual spore formation is likewise inhibited by these elements [39]. The membranes of bacterial cells may be impacted by divalent ions such as Mg which is regarded antibacterial cation where the bacterial membrane's curvature is altered, eventually making the germs more susceptible and increasing the effectiveness of the compounds which affect the membranes, making them more porous [40]. Mg when included in calcium phosphate compound has antibacterial activity against both gram-positive and gram-negative bacteria as well as is efficient against the development of the *C. albicans* fungi cell [41]. The main mechanisms involved in the antimicrobial activities of Mg-based materials have indeed been described as being identical to those seen in other metallic ions. As a result, the literature demonstrated that nanoparticles are often toxic to organisms by causing oxidative stress, inflammation, or even indirect or direct DNA damage, as well as by producing species of reactive oxygen, which cause oxidative DNA damage, lipid peroxidation, and protein denaturation [42]. Thus, both Nd and Mg in the HA structure work synergistically to resist microbes.

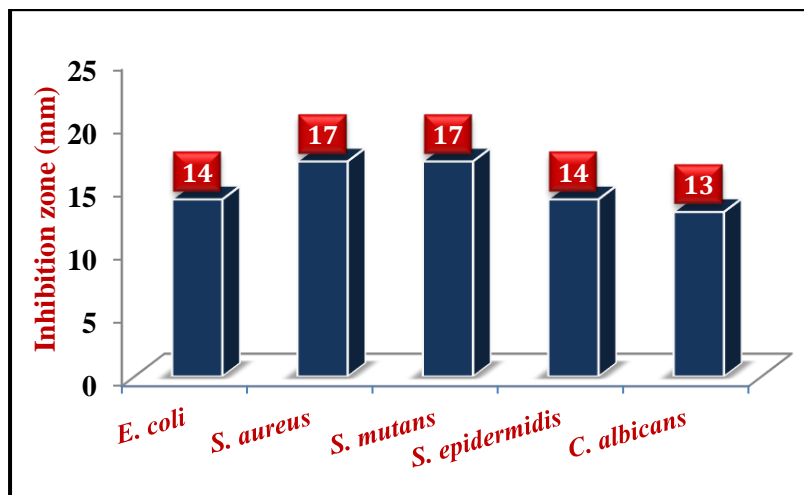


FIG 8: Antibacterial and fungicide activity of Nd-Mg/HA.

3.5. Biocompatibility and cytotoxicity

The results supported previous studies on the biocompatibility of hydroxyapatite in vitro where it is well-known that hydroxyapatite forms direct contact with a bone through the formation of an electron-dense layer at the interface with bone and fibrous tissue without any toxic or harmful effect [43]. The excellent viability of Nd-Mg/HA on the WRL68 cell line was at the concentration of 6.25, 12.50, 25, 50, and 100 $\mu\text{g}/\text{mL}$ with values ranging between $(94.79 \pm 0.61)\%$ to $(71.55 \pm 1.69)\%$.

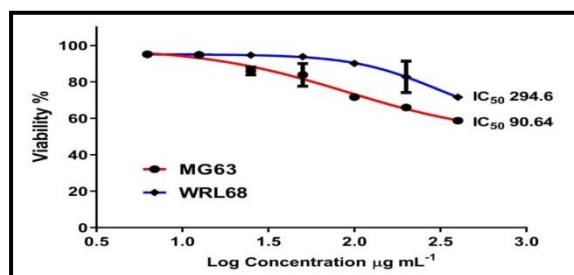
As presented in Table (4) and Fig. (9), Nd-Mg/HA demonstrated high antitumor activity against MG63 cells, where it reduce 41.32 % from the cancer cell compared with 28.45 % of normal cell line at 400 $\mu\text{g}/\text{mL}$. The reduction in the cancer cell line was dose-dependent and the viability arranged between $(95.18 \pm 0.68)\%$ - $(58.68 \pm 1.97)\%$ in a concentration range between (6.25 - 400) $\mu\text{g}/\text{mL}$ for osteosarcoma cells (MG63), while there was slightly effect on WRL68 and the viability ranged from $(94.79 \pm 0.61)\%$ to $(71.55 \pm 1.69)\%$ at

concentrations between 6.25 $\mu\text{g}/\text{mL}$ and 400 $\mu\text{g}/\text{mL}$ and this mean save effect on normal cells. At the same time, the result showed significant differences in IC₅₀ between normal and cancer cells and it was 294.6 $\mu\text{g}/\text{mL}$ and 90.64 $\mu\text{g}/\text{mL}$ for WRL68 and MG63, respectively.

The cytotoxic agents in Nd have anticancer effects; the increased cytotoxicity of these cations is associated with antioxidants, and the activity of the Nd compounds is perhaps related to the coordinative bonds. It is obvious that the presence of neodymium in hydroxyapatite's crystalline structure caused a noticeable antitumor activity. In addition to neodymium's action, the presence of Mg improved the characteristics since Mg has a high biocompatibility with living cells and is essential for bone health by promoting osteoblast proliferation in the early stages of osteogenesis [44]. Mg-substituted HA resembles biological apatite in terms of crystallinity, content, and structure without having any harmful effects [45].

TABLE 4: The effect of Nd-Mg/HA on WRL68 and MG63 cell lines.

Concentration ($\mu\text{g/mL}$)	Viability %			
	MG63		WRL68	
	Mean \pm SD	Sample No.	Mean \pm SD	Sample No.
6.25	95.18 \pm 0.68	3	94.79 \pm 0.61	3
12.50	94.79 \pm 0.61	3	95.10 \pm 0.29	3
25	86.00 \pm 2.14	3	94.64 \pm 0.48	3
50	83.84 \pm 6.21	3	93.87 \pm 1.10	3
100	71.64 \pm 0.42	3	90.08 \pm 1.05	3
200	65.90 \pm 1.77	3	82.74 \pm 8.65	3
400	58.68 \pm 1.97	3	71.55 \pm 1.69	3

**FIG 9:** Cell survival curve of WRL68 and MG63 after treatment with Nd-Mg/HA.

4. CONCLUSION

Substituted hydroxyapatite was successfully prepared by wet chemical precipitation technique, and the results showed that the morphological, crystalline, and chemical properties of the substituted HA have a strong dependency on synthesis parameters, particularly the pH level during the synthesis and the sintering temperature. The results of the FTIR examination indicated the existence of the phosphate, carbonate, and hydroxyl vibrational modes. The particles' sizes ranged from 46 to 88 nm, and their Ca+M/P ratio was 1.64, which is very comparable to that of bone. Also, the biological tests revealed good biocompatibility and antibacterial, antifungal, and anticancer activities. The acquired results lead us to the conclusion that the morphology, crystallinity, chemical properties, and biological activity of the substituted HA can be controlled for particular use as a biomaterial by selecting the proper elements and conditions for preparation.

ACKNOWLEDGEMENTS

The authors are grateful to the University of Technology-Iraq in Baghdad and the Faculty of

Medicine (FOM)/the University of Malaya in Kuala Lumpur.

Funding Statement

The authors received no specific funding for this study.

Declaration of Interest

The authors declare that they have no conflicts of interest to report regarding the present study.

REFERENCES

1. F. M. Chen and X. Liu, "Advancing biomaterials of human origin for tissue engineering," *Progress in Polymer Science*, vol. 53, 2016, doi: 10.1016/j.progpolymsci.2015.02.004.
2. R. A. Anae, "Behavior of Ti/HA in Saliva at Different Temperatures as Restorative Materials," *J. Bio-Tribo-Corrosion*, vol. 2, no. 2, pp. 1–9, 2016, doi: 10.1007/s40735-016-0036-1.
3. J. K. Oleiwi, R. A. Anae, and S. H. Radhi, "CNTs and NHA as reinforcement to improve flexural and impact properties of uhmwpe nanocomposites for hip joint applications," *Int. J. Mech. Eng. Technol.*, vol. 9, no. 11, pp. 121–129, 2018.

4. S. Ponnusamy, R. Subramani, S. Elangomannan, K. Louis, M. Periasamy, and G. Dhanaraj, "Novel Strategy for Gallium-Substituted Hydroxyapatite/Pergularia daemia Fiber Extract/Poly(N-vinylcarbazole) Biocomposite Coating on Titanium for Biomedical Applications," *ACS Omega*, vol. 6, no. 35, pp. 22537–22550, 2021, doi: 10.1021/acsomega.1c02186.
5. A. Mocanu et al., "Ion release from hydroxyapatite and substituted hydroxyapatites in different immersion liquids: In vitro experiments and theoretical modelling study," *R. Soc. Open Sci.*, vol. 8, no. 1, 2021, doi: 10.1098/rsos.201785.
6. A. Dehghanghadikolaei and B. Fotovvati, "Coating techniques for functional enhancement of metal implants for bone replacement: A review," *Materials (Basel)*, vol. 12, no. 11, 2019, doi: 10.3390/ma12111795.
7. T. Tite et al., "Cationic substitutions in hydroxyapatite: Current status of the derived biofunctional effects and their in vitro interrogation methods," *Materials (Basel)*, vol. 11, no. 11, pp. 1–62, 2018, doi: 10.3390/ma11112081.
8. A. Mehatlaf, A. Atiyah, and S. Farid, "An Experimental Study of Porous Hydroxyapatite Scaffold Bioactivity in Biomedical Applications," *Eng. Technol. J.*, vol. 39, no. 6, pp. 977–985, 2021, doi: 10.30684/etj.v39i6.2059.
9. S. Q. Al-Shahrabalee and H. A. Jaber, "Bioinorganic Preparation of Hydroxyapatite and Rare Earth Substituted Hydroxyapatite for Biomaterials Applications," *Bioinorg. Chem. Appl.*, vol. 2023, pp. 1–12, 2023, doi: 10.1155/2023/7856300.
10. S. Panda, C. K. Biswas, and S. Paul, "A comprehensive review on the preparation and application of calcium hydroxyapatite: A special focus on atomic doping methods for bone tissue engineering," *Ceram. Int.*, vol. 47, no. 20, pp. 28122–28144, 2021, doi: 10.1016/j.ceramint.2021.07.100.
11. M. Vidotto et al., "A Comparative EPR Study of Non-Substituted and Mg-Substituted Hydroxyapatite Behaviour in Model Media and during Accelerated Ageing," *Crystals*, vol. 12, no. 2, 2022, doi: 10.3390/cryst12020297.
12. S. Q. Al-Shahrabalee and H. A. Jaber, "Investigation of the Nd-Ce-Mg-Zn/Substituted Hydroxyapatite Effect on Biological Properties and Osteosarcoma Cells," *J. Renew. Mater.*, vol. 11, no. 3, pp. 1485–1498, 2023, doi: 10.32604/jrm.2023.025011.
13. H. H. Bahjat, R. A. Ismail, G. M. Sulaiman, and M. S. Jabir, "Magnetic Field-Assisted Laser Ablation of Titanium Dioxide Nanoparticles in Water for Anti-Bacterial Applications," *J. Inorg. Organomet. Polym. Mater.*, vol. 31, no. 9, 2021, doi: 10.1007/s10904-021-01973-8.
14. K. S. Khashan, F. A. Abdulameer, M. S. Jabir, A. A. Hadi, and G. M. Sulaiman, "Anticancer activity and toxicity of carbon nanoparticles produced by pulsed laser ablation of graphite in water," *Adv. Nat. Sci. Nanosci. Nanotechnol.*, vol. 11, no. 3, 2020, doi: 10.1088/2043-6254/aba1de.
15. K. S. Khashan, B. A. Badr, G. M. Sulaiman, M. S. Jabir, and S. A. Hussain, "Antibacterial activity of Zinc Oxide nanostructured materials synthesis by laser ablation method," in *Journal of Physics: Conference Series*, 2021, vol. 1795, no. 1, doi: 10.1088/1742-6596/1795/1/012040.
16. M. A. Jihad, F. T. M. Noori, M. S. Jabir, S. Albukhaty, F. A. Almalki, and A. A. Alyamani, "Polyethylene glycol functionalized graphene oxide nanoparticles loaded with nigella sativa extract: A smart antibacterial therapeutic drug delivery system," *Molecules*, vol. 26, no. 11, 2021, doi: 10.3390/molecules26113067.
17. O. Kaygili et al., "Structural and Dielectrical Properties of Ag- and Ba-Substituted Hydroxyapatites," *J. Inorg. Organomet. Polym. Mater.*, vol. 24, no. 6, 2014, doi: 10.1007/s10904-014-0074-4.
18. C. Garbo et al., "Advanced Mg, Zn, Sr, Si multi-substituted hydroxyapatites for bone regeneration," *Int. J. Nanomedicine*, vol. 15, pp. 1037–1058, 2020, doi: 10.2147/IJN.S226630.
19. S. Meejoo, W. Maneeprakorn, and P. Winotai, "Phase and thermal stability of nanocrystalline hydroxyapatite prepared via microwave heating," *Thermochim. Acta*, vol. 447, no. 1, 2006, doi: 10.1016/j.tca.2006.04.013.
20. V. Irudhayam and T. Veerabathiran, "Synthesis and Characterization of PVA Assisted Sr-Hydroxyapatite Using Hydrothermal Coupled Microemulsion Method," 2021.
21. Z. Yang, J. Liu, J. Liu, X. Chen, T. Yan, and Q. Chen, "Investigation on physicochemical properties of graphene oxide/nano-hydroxyapatite composites and its biomedical applications," *J. Aust. Ceram. Soc.*, vol. 57, no. 2, 2021, doi: 10.1007/s41779-021-00568-3.
22. M. Andrean et al., "Synthesis of hydroxyapatite by hydrothermal and microwave irradiation methods from biogenic calcium source varying pH and synthesis time," *Boletín la Soc. Española Cerámica y Vidr.*, 2020, doi: 10.1016/j.bsecv.2020.06.003.
23. S. Ferraris et al., "Acta Biomaterialia Bioactive materials: In vitro investigation of different mechanisms of hydroxyapatite precipitation," *Acta Biomater.*, vol. 102, pp. 468–480, 2020, doi: 10.1016/j.actbio.2019.11.024.
24. F. Bollino, E. Armenia, and E. Tranquillo, "Zirconia/hydroxyapatite composites synthesized via sol-gel: Influence of hydroxyapatite content and heating on their biological properties,"

- Materials (Basel), vol. 10, no. 7, 2017, doi: 10.3390/ma10070757.
25. J. Marchi, P. Greil, J. C. Bressiani, A. Bressiani, and F. Müller, "Influence of synthesis conditions on the characteristics of biphasic calcium phosphate powders," *Int. J. Appl. Ceram. Technol.*, vol. 6, no. 1, pp. 60–71, 2009, doi: 10.1111/j.1744-7402.2008.02254.x.
 26. A. Destainville, E. Champion, D. Bernache-Assollant, and E. Laborde, "Synthesis, characterization and thermal behavior of apatitic tricalcium phosphate," *Mater. Chem. Phys.*, vol. 80, no. 1, 2003, doi: 10.1016/S0254-0584(02)00466-2.
 27. R. A. Young and D. W. Holcomb, "Role of acid phosphate in hydroxyapatite lattice expansion," *Calcif. Tissue Int.*, vol. 36, no. 1, 1984, doi: 10.1007/BF02405294.
 28. T. Vijayaraghavan, R. Sivasubramanian, S. Hussain, and A. Ashok, "A Facile Synthesis of LaFeO₃-Based Perovskites and Their Application towards Sensing of Neurotransmitters," *ChemistrySelect*, vol. 2, no. 20, pp. 5570–5577, 2017, doi: 10.1002/slct.201700723.
 29. J. K. Odusote, Y. Danyuo, A. D. Baruwa, and A. A. Azeez, "Synthesis and characterization of hydroxyapatite from bovine bone for production of dental implants," 2019, doi: 10.1177/2280800019836829.
 30. E. Skwarek and D. Sternik, "The influence of the hydroxyapatite synthesis method on the electrochemical, surface and adsorption properties of hydroxyapatite," pp. 20–31, 2017, doi: 10.1177/0263617417698966.
 31. R. M. Ion et al., "Ion-substituted carbonated hydroxyapatite coatings for model stone samples," *Coatings*, vol. 9, no. 4, pp. 1–18, 2019, doi: 10.3390/coatings9040231.
 32. J. F. Cawthray, A. L. Creagh, C. A. Haynes, and C. Orvig, "Ion exchange in hydroxyapatite with lanthanides," *Inorg. Chem.*, vol. 54, no. 4, pp. 1440–1445, 2015, doi: 10.1021/ic502425e.
 33. N. Ekthammathat, A. Phuruangrat, B. Kuntalue, S. Thongtem, and T. Thongtem, "Preparation of neodymium hydroxide nanorods and neodymium oxide nanorods by a hydrothermal method," *Dig. J. Nanomater. Biostructures*, vol. 10, no. 2, pp. 715–719, 2015.
 34. L. Stipniece, K. Salma-Ancane, D. Jakovlevs, N. Borodajenko, and L. Berzina-Cimdina, "The Study of Magnesium Substitution Effect on Physicochemical Properties of Hydroxyapatite," *Mater. Sci. Appl. Chem.*, vol. 28, no. 28, p. 51, 2013, doi: 10.7250/msac.2013.009.
 35. D. N. Ungureanu, D. Avram, A. Catangiu, F. V. Anghelina, and V. Despa, "Characterization of calcium phosphate ceramics obtained by chemical precipitation," *J. Optoelectron. Adv. Mater.*, vol. 17, no. 7–8, pp. 1225–1230, 2015.
 36. A. S. Hammood, "Biomaterialization of 2304 duplex stainless steel with surface modification by electrophoretic deposition," *J. Appl. Biomater. Funct. Mater.*, vol. 18, 2020, doi: 10.1177/2280800019896215.
 37. V. Rodríguez-Lugo et al., "Wet chemical synthesis of nanocrystalline hydroxyapatite flakes: Effect of pH and sintering temperature on structural and morphological properties," *R. Soc. Open Sci.*, vol. 5, no. 8, 2018, doi: 10.1098/rsos.180962.
 38. A. Costescu et al., "Fabrication, characterization, and antimicrobial activity, evaluation of low silver concentrations in silver-doped hydroxyapatite nanoparticles," *J. Nanomater.*, vol. 2013, 2013, doi: 10.1155/2013/194854.
 39. D. E. Talburt and G. T. Johnson, "Some Effects of Rare Earth Elements and Yttrium on Microbial Growth," *Mycologia*, vol. 59, no. 3, 1967, doi: 10.2307/3756768.
 40. K. Demishtein, R. Reifen, and M. Shemesh, "Antimicrobial properties of magnesium open opportunities to develop healthier food," *Nutrients*, vol. 11, no. 10, 2019, doi: 10.3390/nu11102363.
 41. D. Predoi, S. L. Iconaru, M. V. Predoi, M. Motelica-Heino, N. Buton, and C. Megier, "Obtaining and characterizing thin layers of magnesium doped hydroxyapatite by dip coating procedure," *Coatings*, vol. 10, no. 6, 2020, doi: 10.3390/COATINGS10060510.
 42. Y. H. Leung et al., "Mechanisms of antibacterial activity of mgo: Non-ros mediated toxicity of mgo nanoparticles towards escherichia coli," *Small*, vol. 10, no. 6, 2014, doi: 10.1002/sml.201302434.
 43. C. A. van Blitterswijk, S. C. Hesselink, J. J. Grote, H. K. Koerten, and K. de Groot, "The biocompatibility of hydroxyapatite ceramic: A study of retrieved human middle ear implants," *J. Biomed. Mater. Res.*, vol. 24, no. 4, 1990, doi: 10.1002/jbm.820240403.
 44. L. Stipniece, K. Salma-Ancane, N. Borodajenko, M. Sokolova, D. Jakovlevs, and L. Berzina-Cimdina, "Characterization of Mg-substituted hydroxyapatite synthesized by wet chemical method," *Ceram. Int.*, vol. 40, no. 2, 2014, doi: 10.1016/j.ceramint.2013.09.110.
 45. "Landi, E., Logroscino, G., Proietti, L., Tampieri, A., Sandri, M., & Sprio, S. (2008). Biomimetic Mg-substituted hydroxyapatite: from synthesis to in vivo behaviour. *Journal of Materials Science: Materials in Medicine*, 19(1), 239-247."